Environmental Science and Pollution Research (2020) 27:2155–2164
https://doi.org/10.1007/s11356-019-06479-y

RESEARCH ARTICLE

Rhynchosia rufescens AgNPs enhance cytotoxicity by ROS-mediated apoptosis in MCF-7 cell lines

Syed Zameer Ahmed Khader[1] · Sidhra Syed Zameer Ahmed[1] · Gayathri Menon Ganesan[1] · Mohamed Rafi Mahboob[2] · Manimaran Vetrivel[1] · Manavalan Sankarappan[1] · Paulpandi Manickam[3]

Received: 11 February 2019 / Accepted: 9 September 2019 / Published online: 26 November 2019

Abstract

The present study deals with the synthesis of silver nanoparticles (AgNPs) from *Rhynchosia rufescens* and to evaluate its cytotoxic effect mediated through induced apoptosis. The reduction and capping of phytoconstituents was confirmed using FTIR demonstrating O–H and C–H stretching at different peaks. The size and the shape of the particle were determined using scanning electron microscopy (SEM) illustrating 1 μm to 100 nm in size and the composition of compounds in the AgNPs were revealed using XRD and EDX. The results of the antioxidant assays revealed that the synthesized AgNPs had significant radical scavenging potential in dose-dependent inhibition with 22–64% for DPPH and 25–41% for ferric reducing antioxidant power assay at the concentrations of 20–100 μg/ml. Further, the synthesized AgNPs demonstrated potent cytotoxic activity against human breast cancer (MCF-7) cell line with an IC_{50} value of 26 ± 1.0 μg/ml by the MTT assay. Cytotoxicity was confirmed using AO/EtBr and DAPI staining method where nuclear condensation and fragmentation of cancer cells was observed after treatment with nanoparticle. The results were further confirmed by flow cytometry analysis which revealed the occurrence of apoptosis during the S phase in cell cycle exposing the potential of the AgNPs against MCF-7 cancer cell. From the results, we conclude that the synthesized AgNPs from *Rhynchosia rufescens* exhibited multifunctional properties.

Keywords Silver nanoparticles · *Rhynchosia rufescens* · Antioxidant activity · Nuclear fragmentation · DPPH

Introduction

The eco-friendly green synthesis of nanoparticles is a promising field in nanotechnology due to major environmental alarms (Syed Zameer Ahmed et al. 2018a, b). The synthesized nanoparticles offer certain benefits of compatibility for pharmaceutical and other biomedical applications. Nonusage of any toxic chemicals for the synthesis process is more beneficial than physical and chemical methods. These nanomaterials are environment-friendly, cost-effective, and easily scaled up for large-scale synthesis, and in this method, there is no need to use high pressure, energy, temperature, and toxic chemicals (Forough and Farhadi 2010). "Greener synthesis" of nanoparticles has proven to be a better method due to slower kinetics (Elumalai et al. 2010) and has vast and tremendous applications in the field of diagnostics, therapeutics, and antimicrobial catalysis.

There is an urgent need for the development of new medicines with lesser or no side effects and due to the resistance produced by the organisms against the available treatments (Syed Zameer Ahmed et al. 2017, 2019; Poongothai et al. 2011; Sidhra et al. 2019). Nearly 50% of the drugs currently used for medical purposes are from natural sources and almost 63% of anticancer drugs comes from natural resources. Cancer is a leading public health issue with a high mortality around the globe and the most frequently diagnosed cancer in women is breast cancer (Mallath et al. 2014; Jemal et al. 2011). Though there is

Responsible editor: Philippe Garrigues

✉ Sidhra Syed Zameer Ahmed
sidhrazameer@gmail.com

[1] Department of Biotechnology, K.S.Rangasamy College of Technology, K.S.R. Kalvinagar, Tiruchengode, Tamil Nadu 637 215, India

[2] Department of Physics, C. Abdul Hakeem College, Melvisharam, Vellore, Tamil Nadu, India

[3] Department of Zoology, Bharathiar University, Coimbatore, Tamil Nadu, India

a considerable advancement in cancer treatment, requirement for more efficient therapeutics is needed. The development of nanomedicine has evoked researchers to search for a possible therapy using nanomaterials as target drug therapy, which can identify the tumor cells, providing an environment where the healthy cells are not effected by the release of cytotoxic drug (Khan et al. 2012).

Silver is commonly used as the most commercially produced nanoparticles and has vast application in the field of biosensors, medicines, as a detection tool and has been proved to be a potent radical scavenger, antiinflammatory and antiangiogenesis activities (El-Chaghaby and Ahmad 2011), larvicidal activity (Syed Zameer Ahmed et al. 2018a, b), medical device coatings, drug delivery, and personal healthcare products (Mohamed Rafi et al. 2015a, b). Research has proved that silver is extensively used as a potent therapeutic anticancer agent damaging the cell membrane through induced apoptosis and oxidative stress (El-Naggar et al. 2017) with biocompatible and nontoxic nature (Rajan et al. 2015). Many folklore plants with anticancer properties is used for synthesis of silver nanoparticles (AgNPs) as a nanomedicine improving the medicinal efficacy (Gajendran et al. 2014; Kalaiarasi et al. 2015) and research has proved that plant-based AgNPs are effective in treating cancer cells through induce apoptosis, leading the cell to oxidative stress and DNA damage (Vivek et al. 2012). Adverse toxic effects has been observed from the NPs synthesized through physical and chemical methods and to avoid these adverse effects researchers are in search for green synthesis using plant extracts (MeenaKumari et al. 2015).

Rhynchosia rufescens (*Rr*) is one of the tribal pulses widely used in unani, siddha and mostly by tribal community for various ailments. The plant belongs to the family Fabaceae and distributed widely in India, Sri Lanka, Bangladesh, Indonesia, Cambodia, and Malaysia**.** The plant is acknowledged to have high-protein content and it has been used as a folklore medicine (Kalidass and Mohan 2012). Due to lack in the scientific knowledge about the plant and its properties, the present work discusses and validates the anticancerous property of *Rhynchosia rufescens* seed extract and the synthesized AgNPs against MCF-7 breast cancer cell line.

Material and methods

Chemicals and solvents

All the chemicals and solvents were of analytical grade and obtained from Fischer Inorganic and Aromatic Limited, Chennai, India, pre-coated TLC plate with 0.2 mm thick procured from E. Merck, Germany.

Extraction and preparation of AgNPs

Collection and preparation of plant material

The seeds of *Rr* were collected from the hills of Tiruvannamalai, Tamil Nadu, India, shade dried at room temperature, further identified, and authenticated. The dried seeds were coarsely powdered and stored for further use (Ahmed et al. 2016).

Synthesis and characterization of silver nanoparticle

AgNPs were synthesized from the seed powder of *Rr* following the method explained by Syed Zameer Ahmed et al. (2018a, b) with slight modification as follows, 10 ml of the methanol seed extract of *Rr* was added to 90 ml of 2 mM $AgNO_3$ solution and incubated for 24 h. The color of the solution turns to brown color indicating the formation of silver nanoparticles. Further, the synthesized particles were further centrifuged and the pellet was washed with ddH_2O, then with methanol to remove impurities. The resultant pellet was lyophilized under reduced pressure and stored for further usage. The *Rr*-mediated synthesized AgNPs were characterized by FTIR-8400 (Fourier Transform-Infrared Spectroscopy), FE-SEM (Field Emission Scanning Electron Microscopy) with Energy-Dispersive X-Ray Spectroscopy Analyser (EDXA: Oxford Link ISIS-300) and XRD-AXS D8 (Advance X-ray Diffractometer).

In vitro free radical scavenging activity on synthesized AgNPs

DPPH radical scavenging assay

The free radical scavenging ability of any biological material can be assessed using DPPH (2,2-diphenyl-1-picrylhydrazyl) assay. Shimada et al. (1992) method with minor modifications was used to screen the free radical scavenging activity of synthesized AgNPs. The reaction mixture comprises 1.0 mL of AgNPs at varying concentrations (20–100 μg/mL) mixed with 1.0 mL of 0.8 mM/L DPPH solution. The test mixture was incubated under shaking condition for 30 min and then absorbance was noted at 517 nm against gallic acid as control. The inhibition percentage for scavenging of DPPH radical was calculated by the following equation.

$$\%Decolourization = \left[1-\left(\frac{ABS\ \ Sample}{ABS\ \ Control}\right)\right] \times 100$$

Ferric ions (Fe3+) reducing antioxidant power assay

Oyaizu (1986)'s method was followed to carry out ferric ion reducing power of AgNPs with minor modification. 20–100 μg/mL of AgNPs was mixed in 2.5 mL of phosphate buffer (0.2 M, pH 6.6) along with 2.5 mL of potassium ferricyanide 1% ($K_3Fe(CN)_6$) and incubated at 50 °C for 20 min. To the mixture, 10% trichloroacetic acid (2.5 mL) was added and centrifuge at 3000 rpm for 10 min. Finally, to 2.5 mL of supernatant, 2.5 mL of deionized water and 0.5 mL of 0.1% $FeCl_3$ were added. The absorbance at 700 nm was measured against ascorbic acid as positive control.

In vitro anticancer activity for synthesized AgNPs

Cell lines and culturing

The human breast cancer cells (MCF-7) were procured from the National Center for Cell Sciences (NCCS), Pune, India. The cancer cells were maintained in Dulbecco's modified eagles medium (DMEM) added with 2 mM L-glutamine and balanced salt solution (BSS) adjusted to contain 1.5 g/L Na_2CO_3, 0.1 mM nonessential amino acids, 1 mM sodium pyruvate, 2 mM L-glutamine, 1.5 g/L glucose, 10 mM (4-(2-hydroxyethyl)-1-piperazineethane sulfonic acid) (HEPES), and 10% fetal bovine serum (GIBCO, USA). Penicillin and streptomycin (100 IU/100 μg) were adjusted to 1 mL/L. The cells were maintained at 37 °C with 5% CO_2 in a humidified CO_2 incubator.

Evaluation of cytotoxicity

Cell viability of the AgNPs was determined by MTT assay described earlier with slight modification (Rashidi et al. 2016) and the inhibitory concentration (IC_{50}) value was evaluated. MCF-7 were grown separately (1×10^4 cells/well) in a 96-well plate for 48 h in to 75% confluence. The medium was replaced with fresh medium containing serially diluted AgNPs at varying concentrations of 5–80 μg/mL, and the cells were further incubated for 48 h. The culture medium was removed, and 100 μL of the MTT (3-(4,5-dimethylthiozol-2-yl)-3,5-diphenyl tetrazolium bromide) (Hi-Media) solution was added to each well and incubated at 37 °C for 4 h. After removal of the supernatant, 50 μL of DMSO was added to each of the wells and incubated for 10 min to solubilize the formazan crystals. The optical density was measured at 620 nm in an ELISA multiwell plate reader (Thermo Multiskan EX, USA). The OD value was used to calculate the percentage of viability using the following formula.

$$\%\ of\ \ viability = \left[\left(\frac{OD\ \ of\ \ \text{experimental}\ \ sample}{OD\ \ of\ \ \text{experimental}\ \ control}\right)\right] \times 100$$

Morphological observation

The morphological changes in control and AgNP-treated cells were observed using bright field microscopy. The cells were treated with variant concentrations of AgNPs (20, 40, 80 μg/mL) and were allowed to grow on a coverslip for 24 h, fixed with methanol and acetic acid solution and mounted on a glass slide to observe the morphological changes under bright field inverted microscope.

Fluorescence microscopic analysis of nuclear fragmentation and apoptotic cell death

One microliter of dye mixture consist of acridine orange (AO) and ethidium bromide (EtBr) 100 mg/mL each in distilled water was mixed with 90 μL of cell suspension (1×10^5 cells/mL) on clean microscope cover slips. The cancer cells

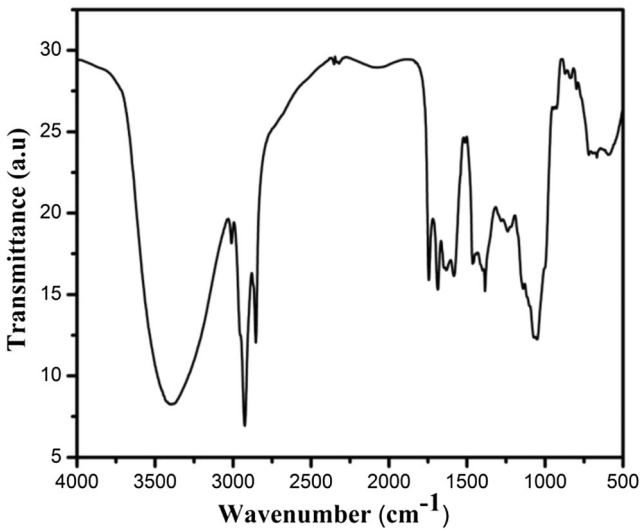

Fig. 1 FTIR spectrum of synthesized AgNPs using extract of *Rhynchosia rufescens*

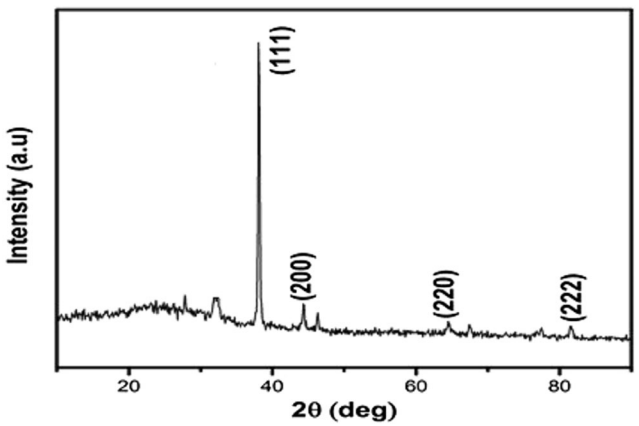

Fig. 2 XRD pattern of synthesized AgNPs using extract of *Rhynchosia rufescens*

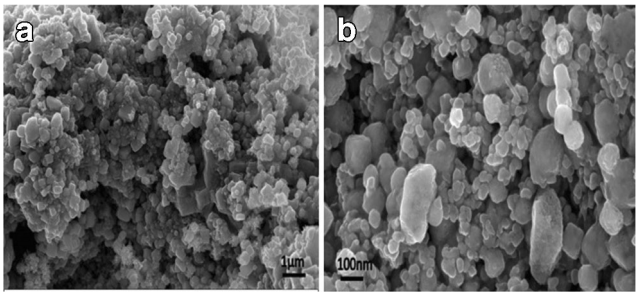

Fig. 3 **a**–**b** SEM micrograph, **a** 1 μm, **b** 100 nm showing the AgNPs using extracts of *Rhynchosia rufescens*

were collected, washed with phosphate buffered saline (PBS) (pH 7.2), and stained with 10 μL of AO/EtBr along with AgNPs at different concentrations (20, 40, 80 μg/mL). After incubation for 2 min, the cells were washed twice with PBS (5 min each) and visualized under a fluorescence microscope (Nikon Eclipse, Inc, Japan) at × 400 magnification with an excitation filter at 480 nm (Liu et al. 2017).

Similarly, the cells were seeded on glass coverslip in a 24-well plate and treated with different concentrations of AgNPs (20, 40, 80 μg/mL) for 24 h. The fixed cells were permeabilized with 0.2% triton X-100 (50 μl) for 10 min at room temperature and incubated for 3 min with 10 μl of DAPI by placing a coverslip over the cells to enable uniform spreading of the stain. The cells were observed under (Nikon Eclipse, Inc, Japan) fluorescent microscope (Chou et al. 2010).

Cell cycle analysis

MCF-7 cells (1×10^5) were seeded in a 96-well plate and incubated for 24-h incubation at 37 °C (5% CO_2), the medium was changed with fresh, supplemented or not (control) with the AgNPs (20–80 μg/mL). After 24-h incubation, cells were harvested with trypsin, washed by PBS, fixed in 70% ethanol, and stored at − 20 °C for 1 h. The cellular nuclear DNA was stained by propidium iodide (PI) followed by removing the ethanol, washed with PBS, the cells were suspended in 0.5 ml PBS containing 50 μg/ml PI and 100 μg/ml RNase and incubated at 37 °C for 30 min. Flow cytometry was performed in duplicate with a BD FACS flow cytometer. From each sample, 10,000 events were collected and fluorescent signal intensity was recorded and analyzed by CellQuest and Modfit.

Statistical analysis

All the *in vitro* experiments were carried out as triplicate and the statistical datas were calucalted using software SPSS version 17.0 and the Graphpad Prism 5 software.

Result and discussion

Green synthesis and characterization of silver nanoparticles

Methanol seed extracts of *Rhynchosia rufescens* were used in the reduction of $AgNO_3$ into Ag^0, and the reduction was initially confirmed by the color change from colorless to yellowish brown. The change in color was observed in UV–Visible spectroscopy which might be due to reduction of silver nitrate by *Rhynchosia rufescens* extract. The sharp peak at 320 nm is assigned to be absorption band of SPR (surface plasmon resonance), due to the combined vibration of electrons of metal nanoparticles in resonance with light wave (Mohamed Rafi et al. 2015a, b). The FTIR spectrum of biosynthesized AgNPs with *Rhynchosia rufescens* is shown in Fig. 1 recorded from 400 to 4000 cm^{-1}. The broad and strong absorbance peak at 3440 cm^{-1} corresponded to O–H stretching followed by a sharp peak at 2946 cm^{-1} which is assigned as C–H stretch respectively (Syed Zameer Ahmed et al. 2018a, b). The significant peaks observed at 1671, 1462, and 1153 cm^{-1} were

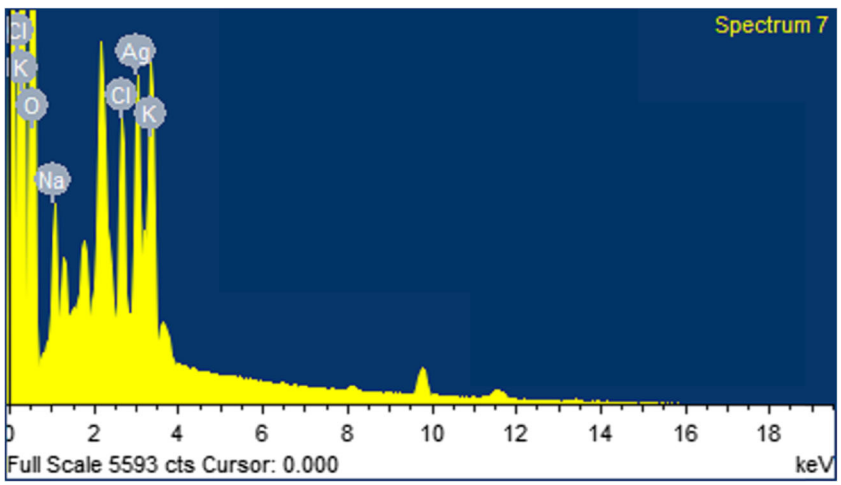

Fig. 4 EDX spectrum of AgNPs synthesized using extract of *Rhynchosia rufescens*

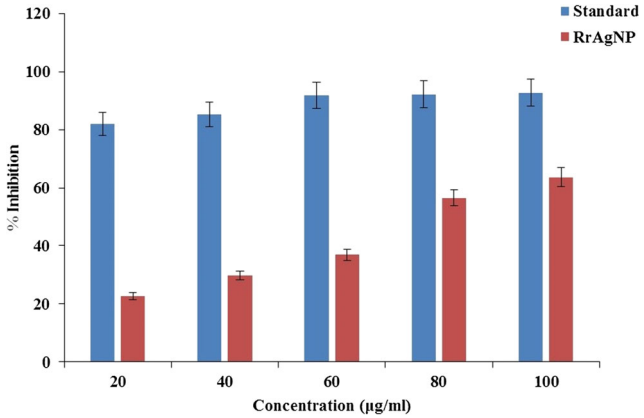

Fig. 5 Effect of synthesized AgNPs on DPPH (2,2-diphenyl-1-picrylhydrazyl) at 20–100 µg/ml concentration

assigned as aldehydes, nitrogen (N–O), and aromatic compounds (C–H), respectively.

The X-ray diffraction pattern of biosynthesized AgNPs is shown in Fig. 2. The highest 2θ peaks observed at 37.6°, 46.5°, 64.3°, and 83.3° correspond to (111), (200), (220), and (222) planes, respectively. The peaks were well matched with JCPDS No. 4-0783. The extra diffraction peaks in the XRD pattern may be due to the crystallization of bio-organic phase in the plant extract (Singh and Jialal 2012). The SEM image in Fig. 3 showed the morphology of biosynthesized AgNPs is nearly spherical shape in the range of 1 µm to 100 nm. Figure 4 shows the EDX spectrum representing the signals as Ag (3 keV), O (0.5 keV), and sodium (1 keV). The spectrum at 3 keV indicates that the Ag has been correctly identified. Generally, Ag nanoparticles show typical optical peak at 3 keV (Syed Zameer Ahmed et al. 2018a, b). The absorption peak of O in EDX spectrum might be due to the involvement of phytocompounds in capping and stabilizing of Ag nanoparticles through O-related groups (Mohamed Rafi et al. 2015a, b).

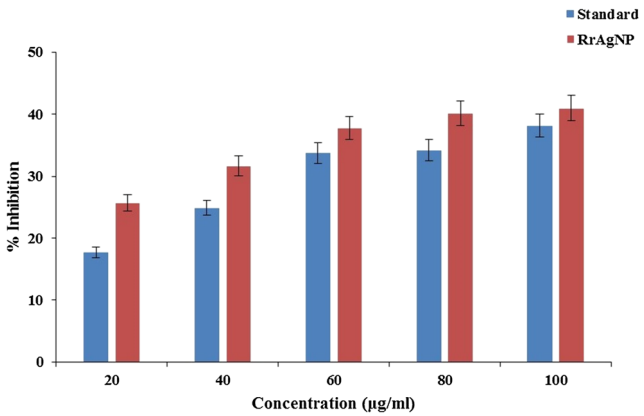

Fig. 6 Effect of synthesized AgNPs on ferric ions (Fe3+) reducing antioxidant power assay (FRAP) at 20–100 µg/ml concentration

In vitro radical scavenging activity of silver nanoparticles

It is evident that free radicals have a major role in pathological conditions in human causing oxidative damage by ROS and RNS released by neutrophil and activated macrophages causing various diseases like cancer, cataracts, diabetes, Parkinson's disease, autism, arthritis, heart disease, Alzheimer's dementia, and even aging (Singh and Jialal 2012; Rege et al. 2012). The effect of these radicals is protected by antioxidant defense mechanism or radical scavenging ability (Das and Roychoudhury 2014). Research has proved that many plant- and microorganism-based products are used as an effective therapeutic agent (Syed Zameer Ahmed et al. 2018a, b). DPPH a nitrogen-centered free radical widely used to test the ability of compounds to act as free radical scavenger (Syed Zameer Ahmed et al. 2018a, b; Sidhra et al. 2017). There was a dose-dependent radical scavenging activity observed with 22.68% at 20 µg/ml concentration; as the concentration increases, scavenging activity improves and maximum activity was observed at 100 µg/ml with 63.68% (Fig. 5). The possible mechanism might be that DPPH accepts the electrons from the AgNPs which is observed with the change in color from violet to yellow (Syed Zameer Ahmed et al. 2018a, b).

Ferric reducing antioxidant power (FRAP) assay is one of the easy and rapid way to evaluate antioxidant activity of any supplements (Preethi et al. 2010). The reducing ability of the synthesized AgNPs from *Rhynchosia rufescens* is represented in Fig. 6 and the results reveal that the activity of synthesized AgNPs were lesser than that of standard, but the increases in concentration reducing ability improve by 25.7 to 40.96% at 20–100 µg/ml concentration (Fig. 6). The reducing ability of the synthesized AgNPs suggests the presence of reductones which donate hydrogen atom and destruct free radical chain formation which could help the body defense mechanism to combat various diseases (Syed Zameer Ahmed et al. 2018a, b).

Cytotoxicity analysis

The changes in the cell morphology of MCF-7 cancer cells after treatment with AgNPs are represented in Fig. 7. The morphological change in the cell plays a predominant role expressing the proliferation inhibition of AgNPs against the cancer cell providing preliminary evidence about the mechanism of cytotoxicity. Healthy cytoskeleton structure was observed in the untreated cells exhibiting the proliferation of cells (Fig. 7a). Moreover, the AgNP-treated cells at different doses showed morphological changes like cell shrinkage, irregular shape, clustering of cells, and blebbing representing cell death in dose-dependent manner (Fig. 7b–d). Similar

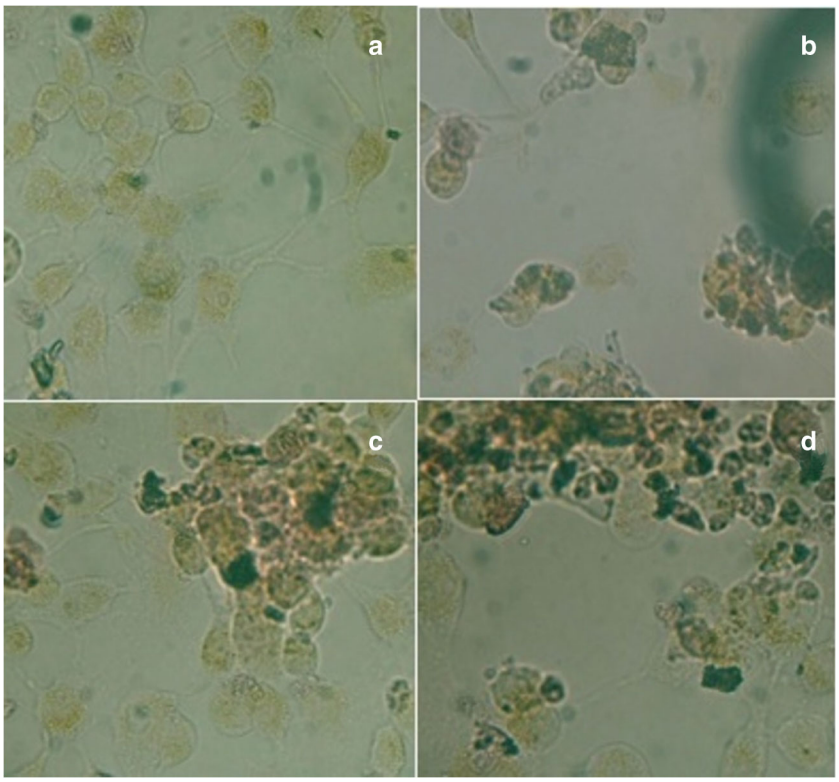

Fig. 7 Images of morphological analysis on human breast cancer (MCF-7) cell line. **a** Control untreated cells, **b–d** AgNP-treated cell at the concentrations of 20, 40, and 80 μg/ml

effects were observed by previous researchers where irregular assembly of microtubule with disruption in cytoskeletal function was observed after treatment (Asharani et al. 2009).

The cytotoxicity effect of AgNPs against MCF-7 cell line was evaluated using MTT assay where growth inhibition was assessed comparing with the standard drug doxorubicin (Fig. 8). Dose-dependent inhibition of cell growth and cell death was observed in MCF-7 cells after treatment with AgNPs. The experimental results demonstrated dose-dependent inhibition of cell proliferation and the IC_{50} value was found to be 26 ± 1.0 (Fig. 8). The study is in agreement with the previous study reporting the activity of AgNPs (Oves et al. 2018; Shaikh et al. 2014).

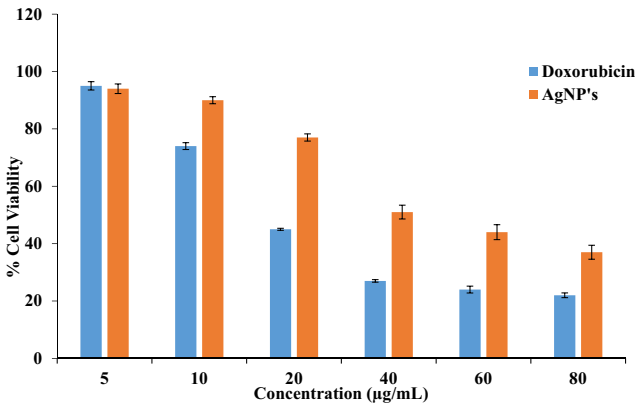

Fig. 8 Effect of synthesized AgNPs on cell viability (MCF-7)

In order to elucidate the apoptotic activity of synthesized AgNPs, apoptotic staining fluorescence microscopic analysis using AO/EtBr staining was performed MCF-7 cell line. In normal cell, the AO dye emits green fluorescence after entering the membrane, whereas, EtBr emits red fluorescence with nonviable cells due to loss of their membrane integrity. Research has proved that apoptosis is defined as programed cell death and degrades cytoplasmic contents in cell organelles (Shaikh et al. 2014). The control cells illustrated green fluorescence (Fig. 9a) but the AgNPs (Fig. 9b–d) cells demonstrated yellow green representing the initial stages of apoptosis and finally illustrating orange/red color representing late-stage process due to the formation of necrosis caused by induced apoptosis and the nuclear condensation effect on the cells due to the addition of AgNPs (Fig. 9). The results are in line with the previous report with the studies carried out with *Phoenix dactylifera* and *Adenium obesum* representing dose-depending apoptosis with fluorescent color change (Shaikh et al. 2014; Liu et al. 2017; Farah et al. 2016).

In order to confirm further, the nuclear condensation and fragmentation of extract and AgNPs with different concentrations (20–80 μg/ml) on selected cancer cells was evaluated using DAPI staining method. DAPI is a blue fluorescent DNA stain illuminates on binding with dsDNA (Chazotte 2011). Fluorescence microscopy images of breast cancer cells after 24 h stained with DAPI in the presence and absence of AgNPs are represented in Fig. 10. It is found that Fig. 10(b–d) AgNP-treated cells shows higher level of nuclear

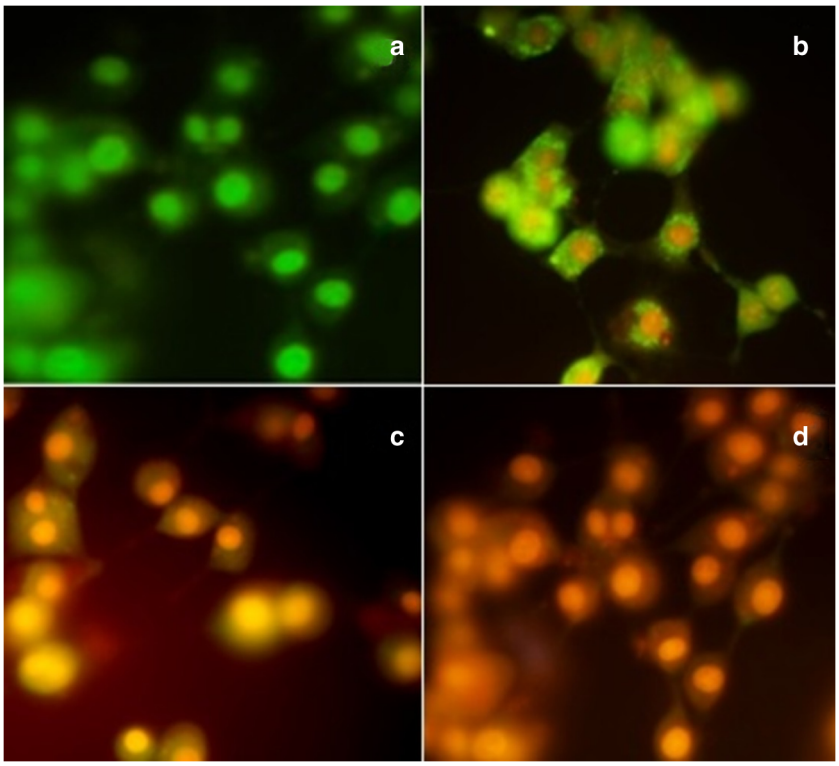

Fig. 9 Images of fluorescent microscopic analysis of AgNPs induced apoptosis in MCF-7 cell with AO/EtBr. **a** Control untreated cells shown in green color, **b**–**d** AgNP-treated cells at the concentrations of 20, 40, and 80 μg/ml; showing apoptotic cells, necrotic cells with orange/red color

fragmentation with bright fetches which indicates the condensed chromatins and nuclear fragmentations in the cancer cells which is not observed in the untreated cells. The nuclear condensation effect was found to be in dose-dependent manner and previous reports stated that human breast cancer cells treated with the extracts of *Astrodaucus persicus* showed potential decrease in the cell proliferation by staining with DAPI (Abdol mohammadi et al. 2008). The anticancer

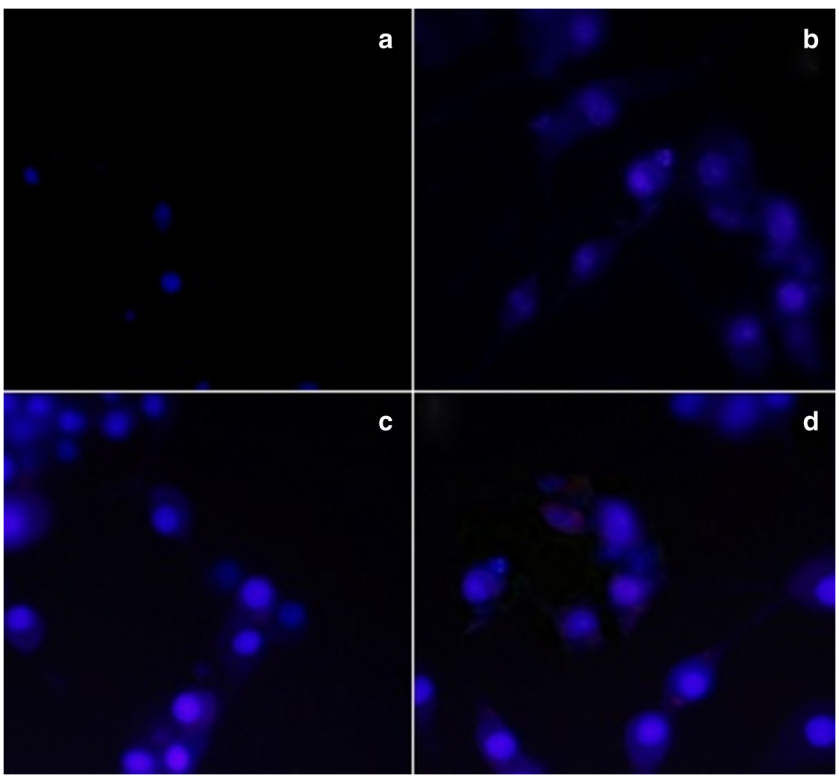

Fig. 10 Effect of AgNPs on nuclear fragmentation in MCF-7 cells by DAPI staining. **a** Control cells, **b**–**d** AgNP-treated cells at the concentrations of 20, 40, and 80 μg/ml; indicates apoptotic cells

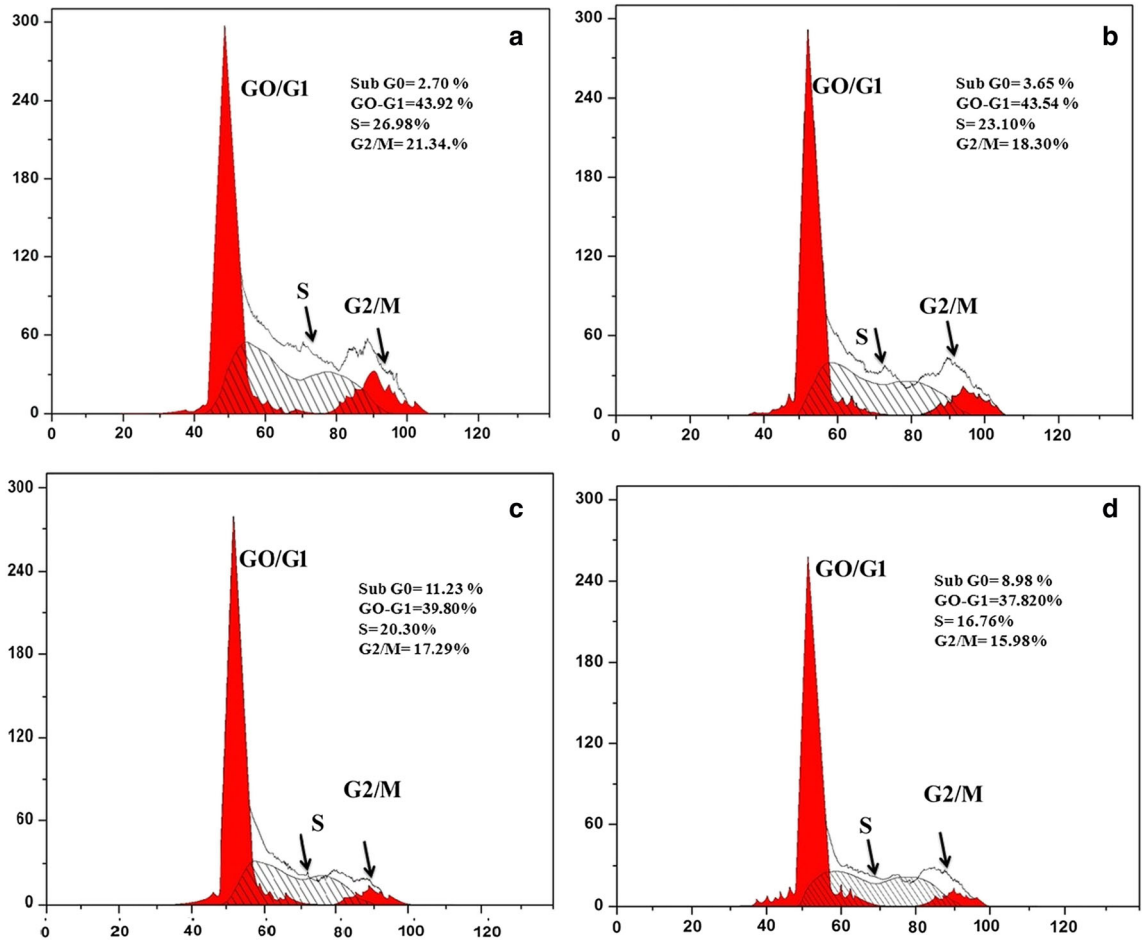

Fig. 11 Effect of AgNPs on cell cycle progression of MCF-7 cells using flow cytometry. **a** Control cells, **b**–**d** AgNP-treated cells at the concentrations of 20, 40, and 80 μg/ml; representing cell cycle arrest in S phase

potential of AgNPs may be due to the production of reactive oxygen species (ROS) from mitochondria inducing the process of apoptosis causing cell death.

The evaluation of anticancer effect induced by AgNPs in MCF-7 cells on cell cycle distribution was carried out by flow cytometric analysis. The proliferation inhibition may stalk from disturbing the cell cycle, to test the hypothesis, cell cycle analyses were conducted after 24-h exposure of the synthesized AgNPs below the IC_{50}, near the IC_{50}, and above the IC_{50} values on MCF-7 cells. As shown in Fig. 11, AgNPs were able to inhibit the cell cycle at various phases. In untreated control, there was an accumulation of cells in G0-G1 phase, whereas, the percentage of cells at the S phase significantly decreased after treatment with AgNPs (Fig. 12). Moreover, the DNA duplication was arrested in respect to the treatment with which is comparable to that of untreated control. From the present results of cytotoxicity and fluorescence analysis, it can be concluded that decrease in the viability of cells in S phase may be due to DNA damage caused by AgNPs leading to death of the cells (Kavithaa et al. 2016).

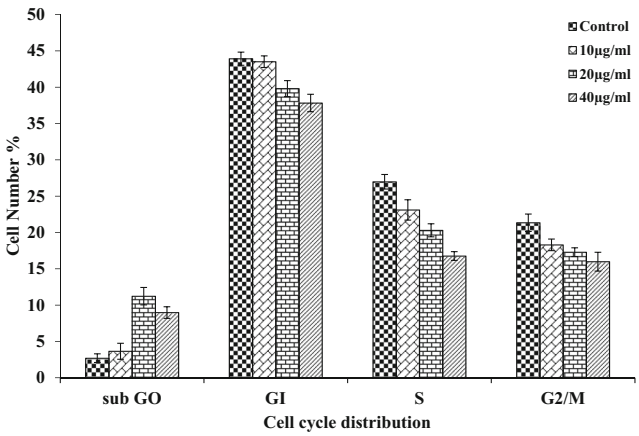

Fig. 12 Cell viability of breast cancer cells (MCF-7) on cell cycle analysis after treatment with AgNPs

The result indicated that the antiproliferative effect of the AgNPs could be predominantly derived from inducing cell cycle arrest mainly in synthetic phase (Loutfy et al. 2015). Thus, from the results from MTT assay and fluorescence microscopy analysis (AO/EtBr and DAPI), it could be confidently reported that the synthesized AgNPs from *Rhynchosia rufescens* help in inhibiting cancer growth; moreover, further research on animal model is required to understand the mechanism.

Conclusion

The present work exemplifies the fast, eco-friendly, and convenient method for synthesizing silver nanoparticle from *Rhynchosia rufescens*. Synthesized AgNPs demonstrated significant antioxidant activity and also exhibited significant cytotoxic affect against human breast cancer cell line (MCF-7) with induced apoptosis and nuclear fragmentation with cell cycle arrest at S phase assessed using flow cytometry. Thus, the findings of our study suggest that the *Rhynchosia rufescens* AgNPs inhibit the growth of cancer cells in *in vitro* model and be developed as an alterative drug for cancer only after further investigations and research on animal model.

Acknowledgments The authors are grateful to the management and Principal of K.S.Rangasamy College of Technology for providing infrastructure to carry out this research work. Authors are thankful to the infrastructure provided by DST-FIST, India, and DBT-STAR Scheme, India.

References

Abdol mohammadi MH, Fouladdel SH, Shafiee A, Amin GH Ghaffari SM, Azizi E (2008) Anticancer effects and cell cycle analysis on human breast cancer T47D cells treated with extracts of *Astrodaucus persicus* (Boiss.) Drude in comparison to Doxorubicin. DARU-Journal of Faculty of Pharmacy 16(2):112–118

Ahmed KSZ, Sidhra S, Ponmurugan P, Senthil Kumar B (2016) Ameliorative potential of *Solanum trilobatum* on oxidative stress in alloxan induced diabetic rats. Pakistan Journal of Pharmaceutical Sciences 29(5):1571–1578

Asharani PV, Low G, Mun K, Hande MP, Valiyaveettil S (2009) Cytotoxicity and genotoxicity of silver. ACS Nano 3(2):279–290. https://doi.org/10.1021/nn800596w

Chazotte B (2011) Labeling nuclear DNA using DAPI. Cold Spring Harbor protocols. https://doi.org/10.1101/pdb.prot5556

Chou CC, Yang JS, Lu HF, Ip SW, Lo C (2010) Quercentin-mediated cell cycle arrest and apoptosis involving activation of a caspase cascade through the mitochondrial pathway in human breast cancer MCF-7 cell lines. Archives of Pharmacal Research 33(8):1181–1191. https://doi.org/10.1007/s12272-010-0808-y

Das K, Roychoudhury A (2014) Reactive oxygen species (ROS) and response of antioxidants as ROS-scavengers during environmental stress in plants. Frontiers in Environmental Science. https://doi.org/10.3389/fenvs.2014.00053

El-Chaghaby GA, Ahmad AF (2011) Biosynthesis of silver nanoparticles using *Pistacia lentiscus* leaves extract and investigation of their antimicrobial effect. Oriental Journal of Chemistry 27:929–936

El-Naggar NEA, Hussein MH, El-Sawah AA (2017) Bio-fabrication of silver nanoparticles by phycocyanin, characterization, in vitro anticancer activity against breast cancer cell line and *in-vivo* cytotoxicity. Scientific Reports 7:10844. https://doi.org/10.1038/s41598-017-11121-3

Elumalai EK, Prasad TNVKV, Hemachandran J, Vivian Therasa S, Tirumalai T, David E (2010) Extracellular synthesis of silver nanoparticles using leaves of *Euphorbia hirta* and their antibacterial activities. Journal of Pharmaceutical Sciences and Research 2:549–554

Farah MA, Ali MA, Chen SM, Li Y, Al-Hemaid FM, Abou-Tarboush FM, Al-Anazi KM, Lee J (2016) Silver nanoparticles synthesized from *Adenium obesum* leaf extract induced DNA damage, apoptosis and autophagy via generation of reactive oxygen species. *Colloids and Surfaces B: Biointerfaces* 141:158–169. https://doi.org/10.1016/j.colsurfb.2016.01.027

Forough M, Farhadi (2010) Biological and green synthesis of silver nanoparticles. Turkish Journal of Engineering and Environmental Sciences 34:281–287. https://doi.org/10.3906/muh-1005-30

Gajendran B, Chinnasamy A, Durai P, Jegadeesh Raman J, Ramar M (2014) Biosynthesis and characterization of silver nanoparticles from *Datura inoxia* and its apoptotic effect on human breast cancer cell line MCF7. Materials Letters 122:98–102. https://doi.org/10.1016/j.matlet.2014.02.003

Jemal A, Bray F, Center MM, Ferlay J, Ward E, Forman D (2011) Global cancer statistics. CA Cancer Journal for Clinicians 61:69–90. https://doi.org/10.3322/caac.20107

Kalaiarasi K, Prasannaraj G, Sahi SV, Venkatachalam P (2015) Phytofabrication of biomolecules coated metallic silver nanoparticles using leaf extracts of *in vitro* raised bamboo species and its anticancer activity against human PC3 cell lines. Turkish Journal of Biology 39:223–232. https://doi.org/10.3906/biy-1406-10

Kalidass C, Mohan VR (2012) Biochemical composition and nutritional assessment of selected under-utilized food legume of the genus Rhynchosia. International Food Research Journal 19(3):977–984

Kavithaa K, Paulpandi M, Padma PR, Sumathi S (2016) Induction of intrinsic apoptotic pathway and cell cycle arrest via baicalein loaded iron oxide nanoparticles as a competent nanomediated system for triple negative breast cancer therapy. RSC Advances 6:64531–64543. https://doi.org/10.1039/C6RA11658B

Khan MI, Mohammad A, Patil G, Naqvi SA, Chauhan LK, Ahmad I (2012) Induction of ROS, mitochondrial damage and autophagy in lung epithelial cancer cells by iron oxide nanoparticles. Biomaterials 33:1477–1488

Liu M, Li R, Tang Y, Chang J, Han R, Zhang S, Jiang N, Ma F (2017) New applications of acridine orange fluorescence staining method: screening for circulating tumor cells. Oncology Letters 13:2221–2229. https://doi.org/10.3892/ol.2017.5724

Loutfy S, Al-Ansary NA, Abdel-Ghani NT, Hamed AR (2015) Antiproliferative activities of metallic nanoparticles in an *in vitro* breast cancer model. Asian Pacific Journal of Cancer Prevention 16:6039–6046

Mallath MK, Taylor DG, Badwe RA, Rath GK, Shanta V, Pramesh CS, Digumarti R, Sebastian P, Borthakur BB, Kalwar A, Kapoor S (2014) The growing burden of cancer in India: epidemiology and social context. Lancet Oncology 15(6):70115–70119. https://doi.org/10.1016/S1470-2045(14)70115-9

MeenaKumari M, Jacob J, Philip D (2015) Green synthesis and applications of Au–Ag bimetallic nanoparticles. Spectrochimica Acta Part A Molecular and Biomolecular Spectroscopy 137:185–192. https://doi.org/10.1016/j.saa.2014.08.079

Mohamed Rafi M, Syed Zameer Ahmed K, Prem Nazeer K, Siva Kumar D, Thamilselvan M (2015a) Antibacterial activity of iron oxide nanoparticles on polysaccharide templates: synthesis, characterization and magnetic studies. Malaysian Polymer Journal 10(1):16–22

Mohamed Rafi M, Syed Zameer Ahmed K, Prem Nazeer K, Siva Kumar D, Thamilselvan M (2015b) Synthesis, characterization and magnetic properties of hematite (a-Fe2O3) nanoparticles on polysaccharide templates and their antibacterial activity. Applied Nanoscience 5:515–520. https://doi.org/10.1007/s13204-014-0344-z

Oves M, Aslam M, Rauf MA, Qayyum S (2018) Antimicrobial and anticancer activities of silver nanoparticles synthesized from the root hair extract of *Phoenix dactylifera*. Materials Science and Engineering: C 89:429–443. https://doi.org/10.1016/j.msec.2018.03.035

Oyaizu M (1986) Studies on product of browning reaction prepared from glucose amine. Japanese Journal of Nutrition 44:307–315. https://doi.org/10.5264/eiyogakuzashi.44.307

Poongothai K, Ponmurugan P, Syed Zameer Ahmed K, Senthil Kumar B, Sheriff SA (2011) Antihyperglycemic and antioxidant effects of *Solanum xanthocarpum* leaves (field grown & in vitro raised) extracts on alloxan induced diabetic rats. Asian Pacific Journal of Tropical Medicine 4(10):778–785. https://doi.org/10.1016/S1995-7645(11)60193-4

Preethi K, Vijayalakshmi N, Shamna R, Sasikumar JM (2010) *In vitro* antioxidant activity of extracts from fruits of *Muntingia calabura* Linn. from India. Pharmacognosy Journal 2(14):11–18. https://doi.org/10.1016/S0975-3575(10)80065-3

Rajan R, Chandran K, Harper SL, Yun S, Kalaichelvan PT (2015) Plant extract synthesized silver nanoparticles, an ongoing source of novel biocompatible materials. Industrial Crops and Products 70:356–373. https://doi.org/10.1016/j.indcrop.2015.03.015

Rashidi M, Ahmadzadeh A, Ziai SA, Narenji M, Jamshidi H (2016) Evaluating cytotoxic effect of nanoliposomes encapsulated with umbelliprenin on 4T1 cell line. In Vitro Cellular & Developmental Biology - Animal 53:7–11. https://doi.org/10.1007/s11626-016-0080-7

Rege A, Juvekar P, Juvekar A (2012) *In vitro* antioxidant and anti-arthritic activities of shilajit. International Journal of Pharmaceutical Sciences and Research 4(2):650–653

Shaikh R, Pund M, Dawane A, Iliyas S (2014) Evaluation of anticancer, antioxidant and possible anti-inflammatory properties of selected medicinal plants used in Indian traditional medication. Journal of Traditional and Complementary Science 4(4):253–257. https://doi.org/10.4103/2225-4110.128904

Shimada K, Fujikawa K, Yahara K, Nakamura T (1992) Antioxidative properties of xanthan on the antioxidation of soybean oil in cyclodextrin emulsion. Journal of Agricultural and Food chemistry 40: 945–948. https://doi.org/10.1021/jf00018a005

Sidhra S, Syed Zameer Ahmed K, Krishnaveni R, Anupriya B, Senthil Kumar B, Kishore R (2017) Modulatory effect of *Leucas aspera* on oxidative stress and glucose metabolism against diabetic complications in experimental rats. International Research Journal of Pharmacy 8(8):27–33

Sidhra S, Syed Zameer Ahmed K, Vanmathi M, Muniraj C, Venkatesan T, Karamchand R, Manimaran V (2019) Antiobesity and antihyperlipidemic effect of *Ixora coccinea* on triton-X100 induced hyperlipidemia in rats- an approach to evaluate asymmetrical temperature distribution analysis using thermography. Chinese Herbal Medicines. 11:326–331. https://doi.org/10.1016/j.chmed.2019.05.006

Singh U, Jialal I (2012) Oxidative stress and atherosclerosis. Pathophysiology 13:129–142

Syed Zameer Ahmed K, Sidhra S, Senthil Kumar B, Thanga Kumar A, Geetha K, Mohamed Rafi M, Ponmurugan P, Kishore R (2017) Modulatory effect of dianthrone rich alcoholic flower extract of *Cassia auriculata* L. on experimental diabetes. Integrative Medicine Research 6:131–140. https://doi.org/10.1016/j.imr.2017.01.007

Syed Zameer Ahmed K, Sidhra S, Jagadeeswari S, Mohamed Rafi M, Kishore R (2018a) A comparative study on larvicidal potential of selected medicinal plants over green synthesized silver nano particles. Egyptian Journal of Basic and Applied Sciences 5(1):54–62. https://doi.org/10.1016/j.ejbas.2018.01.002

Syed Zameer Ahmed K, Sidhra S, Thangakumar A, Sanjeeva N, Senthil Kumar B, Syed Tajudeen S, Ponmurugan P (2018b) Radical scavenging potential, antiinflammatory and antiarthritic activity of isolated isomer methyl-γ-orsellinate and roccellatol from *Roccella Montagnei*. Bulletin of Faculty of Pharmacy, Cairo University 56(1):39–45. https://doi.org/10.1016/j.bfopcu.2018.02.001

Syed Zameer Ahmed K, Sidhra S, Thangakumar A, Krishnaveni R (2019) Therapeutic effect of *Parmotrema tinctorum* against complete Freund's adjuvant-induced arthritis in rats and identification of novel isophthalic ester derivative. Biomed. Pharmacother 112: 108646. https://doi.org/10.1016/j.biopha.2019.108646

Vivek R, Thangam R, Muthuchelian K, Gunasekaran P, Kaveri K (2012) Green biosynthesis of silver nanoparticles from *Annona squamosa* leaf extract and it's *in-vitro* cytotoxic effect on MCF-7 cells. Process Biochemistry 47:2405–2410. https://doi.org/10.1016/j.procbio.2012.09.025